

The Flexibility Test System for Studies of Variable Renewable Energy Resources

Hao Li, *Student Member, IEEE*, Zongxiang Lu, *Senior Member, IEEE*, Ying Qiao, *Member, IEEE*, Baosen Zhang, *Member, IEEE* and Yisha Lin, *Student Member, IEEE*

Abstract—The flexibility of power systems to manage variability and uncertainties is becoming increasingly important as the penetration of variable renewable energy continues to raise. Synergies from all parts of the existing system and new flexibility providers are required to balance demand and supply. However, because of fundamental limitations, existing test systems cannot fully support detailed and realistic studies. To fill this gap, this paper presents a 213-bus benchmark, called the FTS-213 system, dedicated for power system flexibility studies. This system has more than 38% of VRE penetration and includes real data at 15 minutes and 1 minute resolutions. The resources considered in the system cover all aspects of the generation, network, demand, energy storage and market. Specifically, to capture the intrinsic relationship between flexibility and renewable energy accommodation, the system contains integration grids, regional transmission grids and inter-regional tie lines. These assets reflect the full stack of utility-scale integration, transmission and consumption within and among regions. They cover multiple voltage levels, from 110 to 750 kV AC and ± 400 to ± 800 kV DC. The impacts of and the interactions between these flexibility factors are analyzed and three sets of planning results are provided.

Index Terms—test system, flexibility, high penetration of variable renewable energy, unit commitment, planning.

I. INTRODUCTION

THE penetration levels of variable renewable energy (VRE) are increasing rapidly worldwide. For example, the share of VRE in electricity generation has reached over 60% in Denmark. The shares in the United Kingdom, Ireland, German, Portugal, Spain, and Qinghai and Gansu Provinces in China are almost at 20% [1]. The variability and uncertainty of VRE have resulted in difficulties in power systems planning and operations [2], [3]. Therefore, ensuring power systems have adequate flexibility is becoming increasingly important [1], [4]–[6].

We define flexibility as “the ability of a power system to reliably and cost-effectively manage the variability and uncertainty of demand and supply across all relevant timescales, from ensuring instantaneous stability of the power system to supporting long-term security of supply” [1]. And a number of system flexibility studies have been conducted to determine and improve the flexibility of power systems [3], [7], [8]. With

the dramatic increase in VRE share, variations in generation far exceed variations in demand.

Flexibility studies have mainly focused on the issues of VRE accommodation, which can be classified into three categories: evaluation, operation and resource planning. The first is to evaluate the system performance and determine whether VREs are creating issues. The second is to optimize system operation to improve the efficiency, reliability and security with large amounts of VRE integration. The last is to allocate flexibility resources for expected operation scenarios [6]. The common theme of these studies is simply using generation to handle large amount of VRE, which is insufficient. “Combined flexibility – provided by all actors” becomes necessary, which means all parts of the existing system and new resources (such as batteries) need to be integrated to provide flexibility [9].

A key challenge in flexibility studies is the lack of a modern benchmark system to test new algorithms and ideas.

Currently, many test systems are modified from existing benchmarks that were not designed for renewable resources, such as Garver’s 6-bus [10], RTS-79 [11], RTS-96 [12], IEEE-118 [13] and IEEE-300 system [13]. Some researchers use simplified regional systems, such as the CAISO system [14], Finnish system [15], ERCOT system [16], WECC system [17], German system [18] and North Sea Offshore Grid [19].

More recently, systems like the NREL-118 [20], XJTU-ROTS2017 [21], HRP-38 [22] and RTS-GMLC [23] are constructed with a high penetration of VRE to facilitate more targeted studies. However, since these systems are still constructed from older ones, they still have shortcomings with respect to both data and system configurations.

With respect to data, VRE in different areas have different characteristics because of complex meteorological and geographical conditions. Therefore, it is critical to provide high resolution and accurate VRE output powers. However, the XJTU-ROTS2017 system only provides a few weeks of data. The NREL-118, HRP-38 and RTS-GMLC systems provide more VRE output data, but these data are based on simulations from idealized settings and do not capture practical characteristics. With respect to system configuration, the idea of “all hands-on deck” approach to flexibility is not well addressed. Existing systems do not provide flexibility factors and resources that fully cover the generation, network, demand, energy storage (ES) and the market. Researchers then need to modify the system to add flexibility factors in ad hoc manners, leading to difficulties in the comparison of algorithms.

Importantly, the fact that the utility-scale VRE needs to be

H. Li, Z. Lu, Y. Qiao and Y. Lin are with the Department of Electrical Engineering, Tsinghua University, Beijing 100084, China. B. Zhang is with the Department of Electrical and Computer Engineering, University of Washington, Seattle, WA 98195, USA (zhangbao@uw.edu).

Corresponding author: Z. Lu (luzongxiang98@tsinghua.edu.cn). This work is funded by the National Key Research and Development Program of China (Grant No. 2016YFB0900100) and the National Natural Science Fund of China (Grant Nos. U1766201, 51677099).

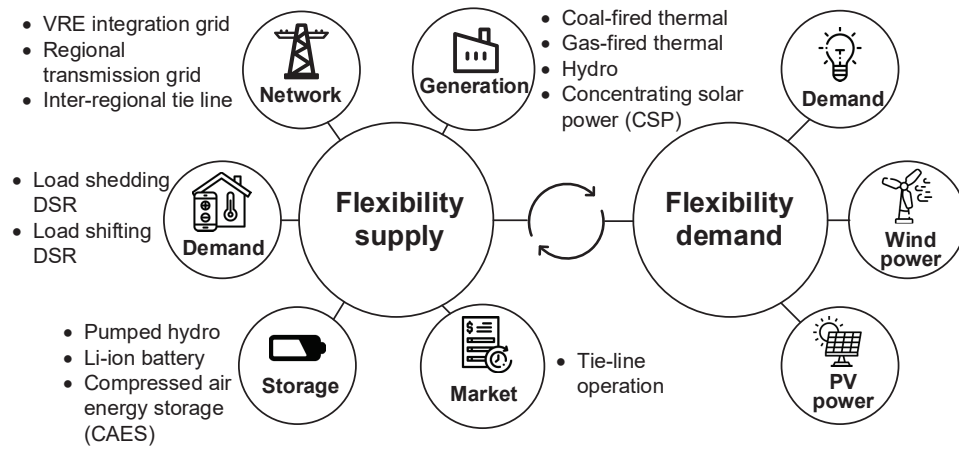


Fig. 1. The balance between flexibility supply and demand.

accommodated by networks with multiple voltage levels is not presented in existing test systems, making a full stack study of distribution and transmission difficult. Unlike traditional thermal and hydro units that directly step-up to the voltage of the bulk grid onsite, wind farms and photovoltaics (PV) stations are connected through an integration grid with multiple voltage conversions (110/220/330 kV) and then reaches a substation at higher voltage levels (500/750 kV). The lower voltage grid may be (and often is, as we show in this paper) the bottleneck in VRE integration, but is typically ignored by existing systems [24], [25].

We propose a new 213-bus test system dedicated to flexibility studies to fill the gaps in the existing test systems. We call it the FTS-213 system (213-bus Flexibility Test System). Network parameters, renewable time series data and the code used in the paper are publicly available and can be found in [26], which can be used for both planning studies and related operational studies. The system is based on a 5-area regional power system in China. New features such as integration grids and DC lines are organically included in our proposed test system since they come from a real grid. Therefore, studies using the proposed system could help researchers understand more clearly how new technologies and algorithms might impact the modern power system performance. The test system has the following features:

- 1) Real, synchronized wind and PV generation data with resolutions of 15 min and 1 min are provided, respectively. There is almost no VRE curtailment in the data.
- 2) Detailed information are provided for generation, network, demand, energy storage and market (as shown in Fig. 1, where DSR stands for demand side response), enabling an integrated analysis of different flexibility factors and coordinated planning of variable flexibility resources.
- 3) VRE integration grids, regional transmission grids and inter-regional tie lines are included, covering the full stack of utility-scale VRE integration, transmission and consumption within and among regions. It has multiple voltage levels from 110 to 750 kV AC and ± 400 to ± 800 kV DC. Compared to other test systems, the

VRE integration grids are unique to our new system. We show the importance of integration grids on VRE accommodation in the case study.

Fig. 1 shows the flexibility factors considered in the system. On the one hand, load demand, wind power and PV power are naturally variable that needs to be balanced, regarded as the flexibility demand. On the other hand, all aspects of the generation, network, demand, energy storage and market provide flexibility. Power plants have traditionally been the main flexibility supply to meet changes in demand. Reinforcement of power grids can alleviate congestion, improve the interconnection between areas to expand the pool of available flexibility resources and manage power flows more efficiently. Demand side response actions can be divided as load shedding and load shifting, with the requirements of the investment in smart grid infrastructure, like smart meters and sensors, and the compensation to the electricity consumers. Storage systems can shift electricity to another duration to provide flexibility. In this test system, the storage includes the pumped hydro, the li-ion battery storage and the compressed air energy storage (CAES). Here market refers to the operation of tie lines between regions. The five areas in the system belong to different stakeholders and the power exchanges between them are relatively small. The tie-line power are scheduled as flat values or preset curves. The flexibility resources considered are the retrofitting of thermal plants and new investments of the other items.

In summary, the contributions of this paper are:

- 1) A 213-bus test system with full network model and high resolution renewable data is provided. Resources covering all the generation, network, demand, energy storage, market operations and VRE integration grids are included. This system allows studies to comprehensively explore how different resources can contribute to diversity. The comparison between the proposed test system and other existing systems is shown in Table I.
- 2) A flexibility study considering the interaction between multiple resources are analyzed. Three sets of results with different VRE penetration, energy storage costs and demand side response costs are provided.

TABLE I
THE COMPARISON BETWEEN TEST SYSTEMS

Test system	VRE time-series data	Flexibility factors							AC power flow support
		Conventional power plants	VRE integration grids	Regional transmission grids	Inter-regional tie lines	DSR	ES	Market	
RTS-79		✓		✓					✓
RTS-96		✓		✓	✓				✓
WECC	✓ unspecified	✓		✓	✓	✓	✓		✓
NREL-118	✓ simulated	✓		✓	✓				
XJTU-ROTS2017	✓ typical weeks	✓		✓	✓				✓
HRP-38	✓ simulated	✓		✓	✓				
RTS-GMLC	✓ simulated	✓		✓	✓		✓		✓
FTS-213 (This paper)	✓ real	✓	✓	✓	✓	✓	✓	✓	

An alternative to using a new system is to modify an existing system. This is simple and can provide valuable information, but the structure of the existing benchmarks are fundamentally limiting to how much it can change. Many of the existing benchmarks originated from systems designed decades ago, like IEEE-118 and IEEE-300 system [20], [27]. These systems are realistic reflections of the grid at those times, but newer systems have qualitatively different features, like the VRE integration grid discussed above and DC lines. For example, the placements of DC lines in actual system (like the one described in this paper) are carefully decided [28]. However, if one uses an IEEE test system, the placement of the lines are almost always done in ad hoc or arbitrary fashions.

The remainder of the paper is organized as follows. Section II introduces the general profile of the FTS-213 system. Section III, IV and V present the data of generation, network and demand side, respectively. In Section VI, the flexibility factors and resources are analyzed. In Section VII, the impact of flexibility factors is explored, and the flexibility resource planning results are provided. The discussions are presented in Section VIII and the conclusions are drawn in Section IX.

II. PROFILE OF THE FTS-213 SYSTEM

The FTS-213 system is extracted from a regional power system in China and is represented as a 5-area system with 213 buses. Each area has 26 to 50 buses. The layout of the system is shown in Fig. 2 and the basic parameters are shown in Table II. In the table, the ‘external peak load’ means the peak power transmitted to the external power systems, ‘conventional generators’ are thermal and hydro power units and ‘VRE’ includes wind, PV and concentrated solar plants (CSP).

TABLE II
BASIC PARAMETERS OF FTS-213 SYSTEM

Parameters	Value
Number of conventional generators	367
Number of branches	422
Voltage levels (kV)	AC:110, 220, 330, 500, 750 DC:±400, ±800
Local peak load (GW)	121.97
External peak load (GW)	45.43
Conventional unit capacity (GW)	187.84
VRE unit capacity (GW)	116.12

The system has abundant renewable energy resources. The total generation capacity is 303.96 GW, of which the VRE

capacity accounts for 38.20%. The total load is 167.40 GW, with 45.43 GW transmitted to external power systems. There are 422 branches (lines and transformers) in the system. VRE integration grids, regional transmission grids and inter-regional tie lines are all included, with voltage levels ranging from 110 to 750kV AC and ±400 to ±800kV DC.

III. SUPPLY SIDE DATA

A. Generation Technology

There are six types of generation units in the system: coal-fired thermal power, gas-fired thermal power, hydropower, wind power, PV power and CSP. As can be seen in Fig. 3, the capacity is abundant in each area and different areas show different characteristics in the generation mix.

The units are described by following parameters: unit capacity (MW), minimum stable power ratio (%), maximum ramp-up rate (MW/min), maximum ramp-down rate (MW/min), minimum up time (h), minimum down time (h), forced outage rate (%), mean time to failure (MTTF, h), mean time to repair (MTTR, h), scheduled maintenance (weeks/year), startup cost (M\$), fixed cost (M\$/(MW·year)), and marginal cost (\$/MWh).

Hydro plants in the test system are reservoir-based plants. Different from the run of river plants, reservoir-based plants can be dispatched to a large extend. Since the capacities of hydro plants are large, we assume the plants can be described by expected output, monthly average output and forced output [20], [22]. Expected output and forced output act as limits on the maximum and minimum output of the plant. The monthly average output constrains the total energy output of hydro units during a month.

A CSP plant is composed of three components, namely solar field, thermal energy storage (TES), and power block. The solar field, concentrating solar irradiation to generate thermal power, is sized by a parameter called the solar multiple (SM), which normalizes the size of the solar field with respect to the power block. The TES is sized by the number of hours that TES can be discharged at its rated capacity. In the system, the SM is set as 2.4 and the TES is set as 10 h [29].

The regulation abilities of thermal, hydro and CSP units are summarized in Table. III. The maximum ramp up/down rate in the table is represented by the ratio of a unit actual ramp rate value compared to its capacity. Since hydro units are constrained by forced output indicator, it is assumed online

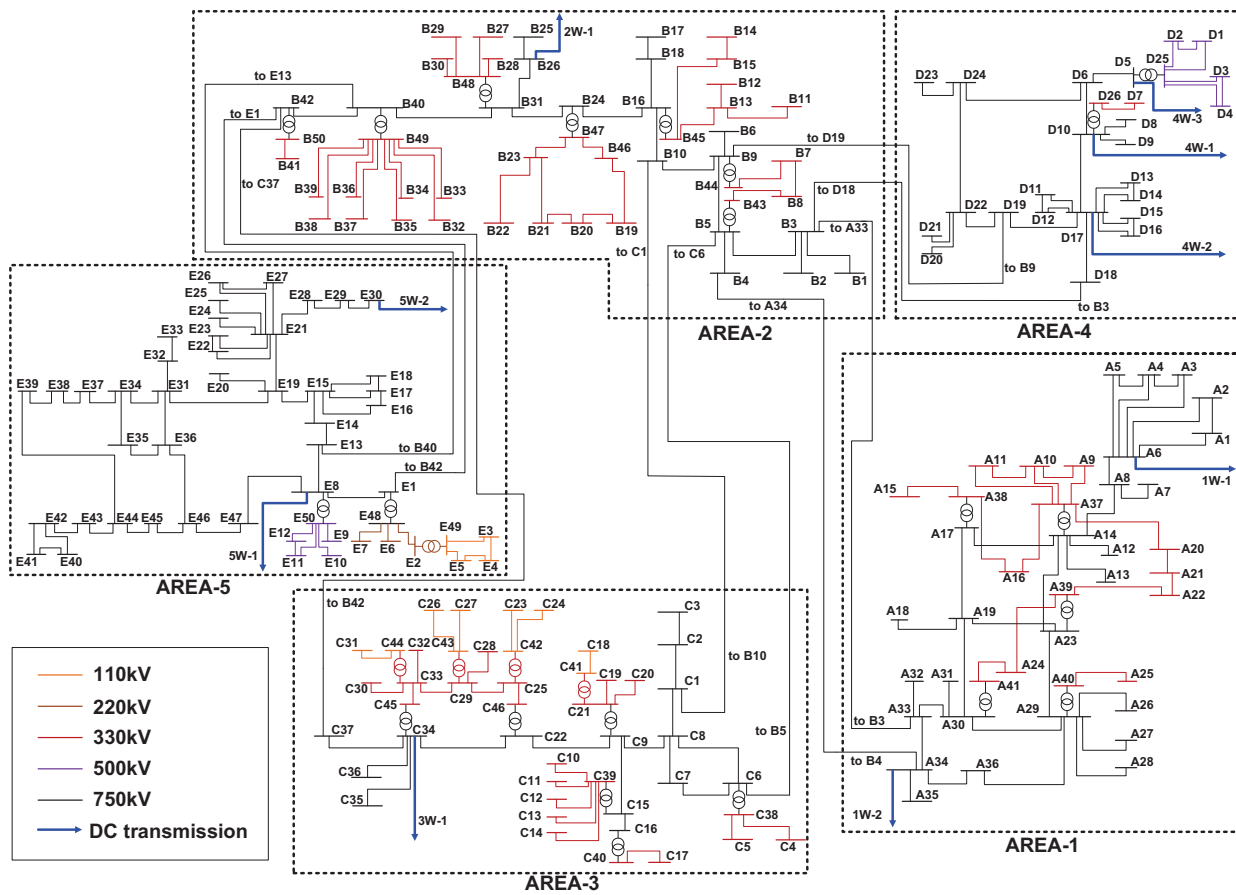


Fig. 2. The topological structure of the FTS-213 system.

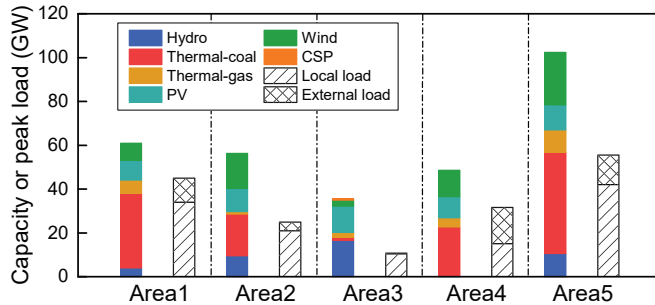


Fig. 3. The generation capacity and peak load in each area.

during the whole year. For further studies like generation expansion planning, we also provide the candidate generators with investment parameters in the dataset [26].

TABLE III
REGULATION ABILITIES OF UNITS

Parameter	Value			
	Coal*	Gas*	Hydro	CSP
Minimum stable power	50~55%	40%	-	40%
Maximum ramp up/down rate	1.5~2%	4%	12.5%	1%
Minimum up/down time	8~12 h	3 h	-	2 h

*'Coal' and 'gas' represent the types of thermal power.

B. VRE Time Series Data

To reflect the variability from the sub-hourly scale to seasonal scale, we provide VRE output time series with the resolutions being 1 min for PV data and 15 min for wind data. Each region has its own wind and PV output time series for the whole year. Distinguish from the previous test systems, in which the VRE time series data is based on simulations, the data in our system is extracted from the practical cases. Wind and PV outputs are derived from VRE plants and small regions with little VRE curtailment in Ningxia and Gansu provinces in China, thus they can reflect the real variability compared with the simulated data.

Fig. 4 shows the VRE hourly variability represented by typical days, which are obtained by the k-medoids method as described in Section VIII. Note that we use the cluster method here to show the variability in some typical days. It can be seen that the ramping events are frequent and the VRE power difference between adjacent hours can achieve 50% of the capacity. Fig. 4 (b)-(d) show the load, wind and PV output of the typical days in Area 1. The ramping events are frequent and the VRE power difference between adjacent hours can reach 50% of the capacity, as the black thick line in Fig. 4 (c) shows. The daily VRE peak-valley difference is also obvious, especially for PV output, reaching 80% of the capacity. Fig. 5 shows the VRE daily variability represented by daily mean output power. The mean power of the continuous days varies

from nearly maximum value among the year to almost zero, as highlighted by dashed boxes in Fig. 5. Fig. 6 shows the VRE monthly variability represented by monthly mean output. Both wind and PV power show seasonal variability. Wind power peaks in spring and winter while reaches valleys in summer and autumn. The variability of PV power is not as obvious as that of wind, but still shows a downward trend in winter. For CSP, the field thermal power produced is generated by

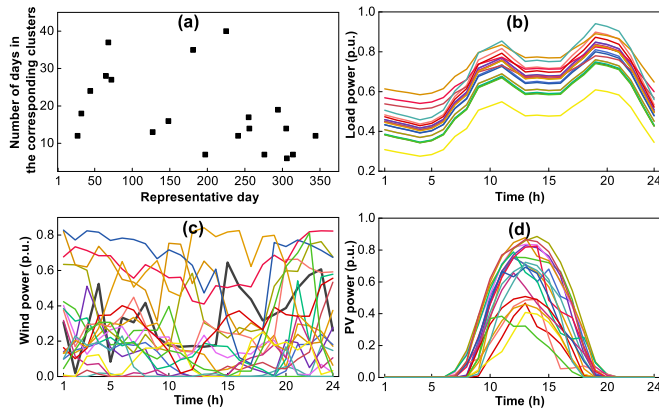


Fig. 4. Representative days with the corresponding number of days and load, wind and PV output power for Area 1.

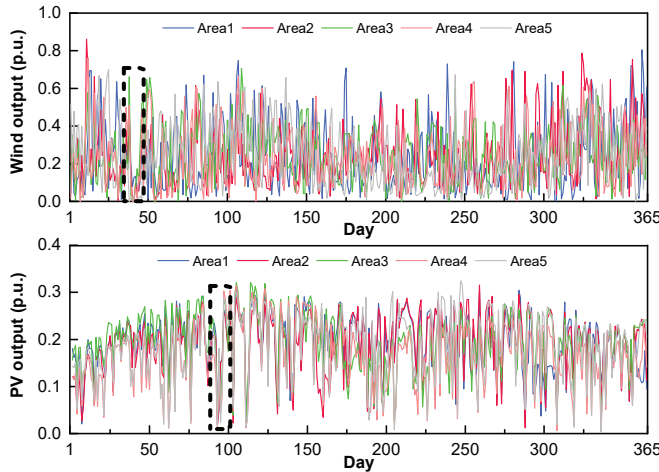


Fig. 5. Daily mean output power of VRE. Dashed boxes include days with almost zero power output.

the Solar Advisor Model and normalized by the power block capacity [30]. The data is in the system database.

IV. TOPOLOGY AND GRID DATA

A. Topology

As shown in Fig. 2, the system has the following characteristics in topology:

1) The system consists of VRE integration grids, regional transmission grids and inter-regional tie lines, with voltage levels from 110 kV to 750 kV. Since VRE resources are spread out in a large area, the integration grid is needed to collect the resources and up-convert the voltages consistent with other

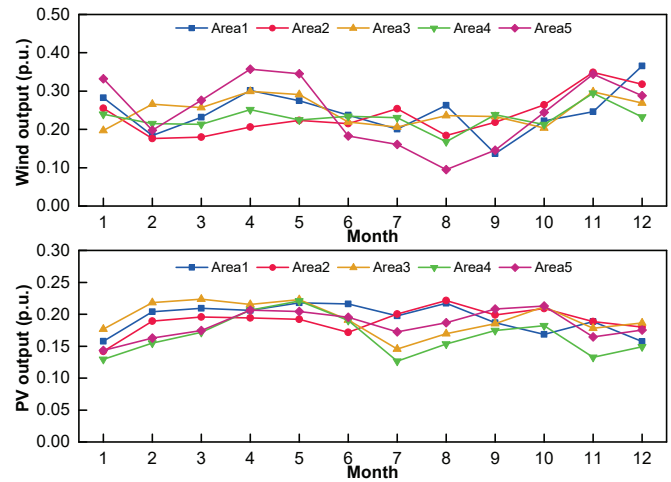


Fig. 6. The monthly average output power of VRE.

buses. Then power is transmitted by regional grids and inter-regional tie lines to meet the electricity demand in all of the regions. An indicator that represents branches belonging to whether VRE integration grids, regional transmission grids or tie lines is presented in the database. The distribution networks in the demand side are aggregated as buses.

2) The typical integration grids are shown in Areas 2 and 3 in Fig. 2. In Area 2, the integration grids in the radiation form are connected to buses B31 and B40, while the grid in the loop form is connected to the bus B24. In Area 3, the integration grid is connected simultaneously to buses C22 and C34.

3) The regional transmission grids, composed of partly 330 kV and 750 kV lines in the system, show different characteristics in different areas. In Areas 1, 4 and 5, they are connected as one or several loops whereas in Areas 2 and 3, they are connected as chains.

4) Among the five areas, Area 2 connects all the other areas directly. All tie lines are under 750kV and provide large transmission capacity between regions.

5) Based on the actual system, all areas transmit power to external systems for the VRE accommodation. The lines connecting to external systems are represented by arrows labeled 'aW-b' in Fig. 2, where 'a' represents the area number and 'b' represents the sequence number of lines connecting to external systems. These lines are under ± 400 and ± 800 kV and are simplified as extra loads on the connected buses.

B. Branch Characteristics

There are 422 branches in the test system. The location of the terminal buses, length (km), reactance (p.u.), resistance (p.u.), charging susceptance (p.u.) and capacity (MW) are provided. The values of these parameters are extracted from the dataset in the State Grid Economic and Technological Research Institute. Reliability parameters involving the outage rate (outages/year) and the outage duration (h) are also included in the database, based on the reports from the China Electricity Council [31]. The reference capacity is 100 MVA

and the reference voltages for 110, 220, 330, 500 and 750 kV are 115, 230, 345, 525 and 788 kV, respectively.

Besides, 133 AC candidate lines and transformers and 36 DC candidate lines are provided and summarized in Table. IV. Both AC and DC candidate branches involve lines or transformers functioning as VRE integration grids, regional transmission grids and inter-regional tie lines. Assume that all the DC candidate lines are VSC-HVDC that can flexibly control the active power and thus provide flexibility to the system. The capital costs of candidate lines are estimated based on [32].

TABLE IV
CANDIDATE LINES AND TRANSFORMERS

		number	capital cost (M\$)
AC candidate	lines	108	19~571
	transformers	25	5~31.5
DC candidate	lines	36	862~1018
	branches		(includes converters)

V. DEMAND SIDE DATA

A. Peak Load and Load Distribution

There are two kinds of load in the system, i.e., local load and external load, with the peak values being 122.47 GW and 45.30 GW, respectively. The local load participation factors are normalized by area, while the external load is represented by the absolute value. Table. V summarizes the load characteristics by area.

TABLE V
LOAD CHARACTERISTICS IN EACH AREA

Area	A.1*	A.2*	A.3*	A.4*	A.5*
Local peak load (GW)	33.95	20.96	10.39	15.10	42.07
Load participation factor	0.2	0.1	0.6	0.6	0.2
	~13.6%	~17.9%	~20.9%	~26.4%	~11.6%
External peak load (GW)	11.00	4.00	0.48	20.00	20.00

*‘A.’ is the abbreviation of ‘Area’.

B. Load Profile

The 8760 hourly time-series data of the local load in each area are adopted from [22]. The external load, according to the annual operation report of the real system, varies with months and the monthly peak power is shown in Fig. 7. From July to December, some of the external load shows a downward trend, since the dominant wind power generally reaches the valley.

VI. FLEXIBILITY RESOURCES AND FACTORS

According to [4], the power system flexibility comes from power plants, grids, DSR, storages and markets. The costs of the flexibility resources are listed in Table. VI.

Improving the trade between regions is an important mechanism for increased flexibility [5]. Nowadays, because of the gap between stakeholders, the power exchange between regions is relatively weak and the tie-line power are scheduled as

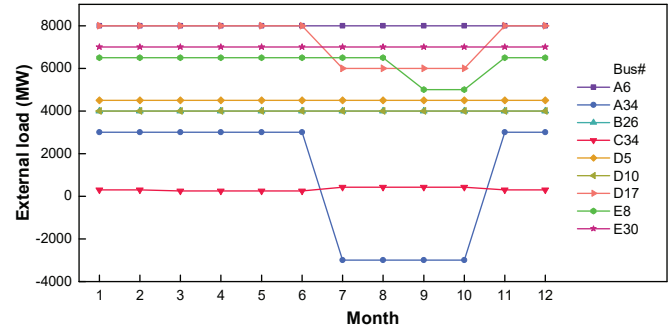


Fig. 7. Monthly external load with the corresponding buses.

TABLE VI
COST OF FLEXIBILITY RESOURCES

Flexibility resources	Investment cost (k\$/MW)	Compensation cost (\$/MWh)
Coal-fired thermal unit retrofit*	30.0 [33]	-
Gas-fired thermal unit retrofit*	200.0 [33]	-
Load shedding excavation	14.3 [34]	64.3 [34]
Load shifting excavation	11.4 [34]	50.0 [34]
Pumped hydro**	2638.0 [35]	-
Li-ion Battery storage**	828.0 [36]	-
CAES**	2544.0 [35]	-

*Only the decrease in minimum stable level is considered here for plants retrofit since lower turndown capability was found to have the most beneficial impact on the system [33].

**The Pumped hydro, battery storage and CAES is assumed as a 16-hour, 4-hour and 16-hour device that would be able to discharge at rated power capacity for 16, 4 and 16h, respectively.

flat values or a preset curves. The tie-line power is regarded as a boundary condition when doing regional power scheduling, sometimes called “*tie-line operation constraints*”. Fig. 8 shows the monthly power exchange between areas in the test system according to the regional practical operation report. If the trade between regions can be promoted and economic dispatch can be implemented among regions, such a constraint can be relaxed.

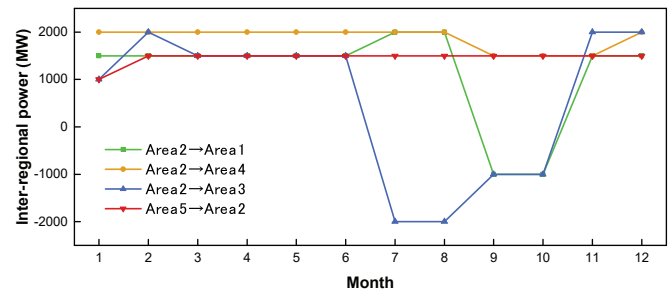


Fig. 8. Power transmission between areas.

VII. BENCHMARK RESULTS OF FLEXIBILITY EVALUATION AND OPTIMIZATION

In this section, the flexibility evaluation is conducted with unit-commitment (UC) based operation simulations and the

flexibility optimization schemes are proposed based on the coordinated flexibility resources planning. Note that the aim of the case study is to show the feasibility of the system and some examples of typical flexibility studies that can be conducted on the proposed test system, so some modeling methods are simplified. Further detailed modeling is also feasible based on our dataset. Also note that the case study conducts simulations on the hourly scale, since a higher resolution data is also provided, the studies with a sub-hourly scale can also be conducted.

A. Model Formulation

1) *UC Based Operation Simulation Model*: A UC based operation simulation model is adopted to enable the analysis of flexibility with regard to unit startup and shutdown. Since there are nearly 400 conventional units in the system, for computation efficiency, we adopt the one-binary-variable UC model [37] that only uses one set of binary variables to represent the unit statuses, i.e., on/off, startup and shutdown. We modified the objective function and startup cost constraints as:

$$\min F_s = \sum_{t=1}^T \sum_{g \in \Omega^G} c_g^G P_{g,t,s}^G + \sum_{t=2}^T \sum_{g \in \Omega^G} C_{g,t,s}^{ST} + \sum_{t=1}^T \sum_{n \in \Omega^N} \beta^L P_{n,t,s}^{L,C} \quad (1)$$

$$s.t. \begin{cases} C_{g,t,s}^{ST} \geq (u_{g,t,s} - u_{g,t-1,s}) c_g^{ST} \\ C_{g,t,s}^{ST} \geq 0 \end{cases} \quad (2)$$

where s, g, t, n represent the selected day, conventional unit, time and bus, respectively. T represents the total time slides in a day. Ω^G represents the set of conventional units. c_g^G and $P_{g,t,s}^G$ represent the marginal generation cost and the power generation of conventional units. $C_{g,t,s}^{ST}$ denotes the startup cost. $P_{n,t,s}^{L,C}$ and β^L represent the load shedding and its unit penalty. $u_{g,t,s}$ represents the on/off status of a unit. c_g^{ST} denotes the unit startup cost.

For branches, the DC power flow model is used with the following constraints:

$$P_{l,t,s} = (\theta_{n^{l+},t,s} - \theta_{n^{l-},t,s}) / x_l \quad (3)$$

$$-P_l^{\max} \leq P_{l,t,s} \leq P_l^{\max} \quad (4)$$

where $P_{l,t,s}$ is the power flow on the branch l at time t in the day s ; θ is the phase angle of the node; n^{l+} and n^{l-} are the start node and end node of branch l ; x_l is the reactance of branch l ; P_l^{\max} is the capacity of branch l .

For hydro plants, the monthly hydro generation energy is divided into daily energy constraints based on the daily mean load. CSP is modeled as in [29].

2) *Coordinated Flexibility Resource Planning Model*: In this part, we build the planning model to optimize the flexibility resources in all the aspects of generation, network, demand and storage. The model is under a two-stage stochastic optimization framework, with the first stage constraining investment decisions and the second stage constraining the

operation simulation of each representative day [22]. This model determines the optimal allocation of multiple flexibility resources under a given renewable capacity penetration, rather than the optimal allocation of generation, transmission, demand and energy storage for a future power system. Thus, we do not consider the increase in demand and the expansion of conventional units is not needed since they are already adequate in the existing system. Similarly, we use the cluster method mainly to show the feasibility of flexibility resource planning in the case study considering computational efficiency. The objective is the summation of annual investment cost and operation cost:

$$\min \sum_{i \in \Omega^F} C_i^{INV} + \sum_{s=1}^{N^S} \rho_s C_s^{OPR} \quad (5)$$

where i represents a flexibility resource and Ω^F represents the set of flexibility resources. N^S is the number of typical days. ρ_s denotes the number of days in a cluster and C_s^{OPR} represents the operation cost in a typical day, which contains the electricity generation cost, load loss penalty, VRE curtailment penalty, and DSR compensation cost.

The constraints in the first stage involve the maximum capacity that could be invested for each flexibility resource and the total budget for the investment.

The constraints in the second stage include the power balance for each node, the system reserve constraints, the operation constraints of the conventional units, renewable power plants, ES, DSR and the power flow of existing and candidate lines [22]. For AC lines the DC power flow is used. For DC lines the power flow is modeled as an adjustable variable to reflect its controllability [22]. Assume that the tie-line operation constraint is relaxed so that new tie lines have a chance to be built. The ES is modeled as in [38] to avoid binary variables. We have also provided efficiency data of ES that facilitate a detailed model. Two types of DSR are modeled as follows:

$$P_{n,t,s}^L = P_{n,t,s}^{L0} - P_{n,t,s}^{SHED} - P_{n,t,s}^{SHIFT} \quad (6)$$

$$\begin{cases} 0 \leq P_{n,t,s}^{SHED} \leq \bar{P}_n^{SHED} \\ \underline{P}_n^{SHIFT} \leq P_{n,t,s}^{SHIFT} \leq \bar{P}_n^{SHIFT} \\ \sum_{t=1}^T P_{n,t,s}^{SHIFT} = 0 \end{cases} \quad (7)$$

where $P_{n,t,s}^{L0}$ and $P_{n,t,s}^L$ represent the load power before and after demand response, respectively. $P_{n,t,s}^{SHED}$ and \bar{P}_n^{SHED} represent the load shedding and its maximum value, which is determined by the capacity of this type of DSR being deployed. \underline{P}_n^{SHIFT} , \bar{P}_n^{SHIFT} and \underline{P}_n^{SHIFT} denote the load shifting, its maximum value and its minimum value. The model is formulated as a mixed integer linear programming problem.

The representative days are selected by the k-medoids clustering method to represent the whole year. The clustering is based on the dominant daily load, wind power and PV power curves, whose results are shown in Fig. 4 (a). Note that the clustering is used to reduce the number of daily

profiles and does not change the temporal resolution of the data. Since the profiles of VRE and load for some days are similar, clustering is a widely used way to analyze the whole year's performance. We agree that some information will be lost after clustering, while we use the cluster method mainly to estimate the production cost and VRE accommodation in the case study of flexibility resource planning considering computational efficiency.

B. Operation Simulation Results

Based on the UC model in Section VII-A1), a day-by-day operation simulation is conducted. The daily production costs are shown in Fig. 9, showing that they have a similar fluctuation with the demand. No load shedding occurs during the whole year. Fig. 10 shows the generation stack of the full system for the days with maximum daily load, maximum daily wind generation and maximum PV generation, respectively. The overall generation mix is generally consistent with that of the real system.

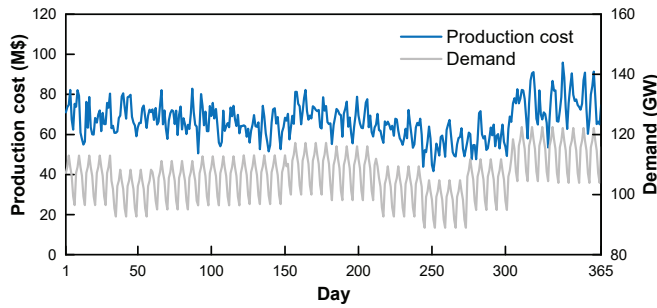


Fig. 9. Daily production costs and daily average demand.

C. Flexibility Evaluation

1) *Case Setting*: In this part, we investigate the impact of factors related to power system flexibility, using the model in Section VII-A1). These factors include ramping rate, minimum stable level, minimum up/down time of conventional units, VRE integration grid capacity, regional transmission capacity, inter-regional tie-line capacity and inter-regional exchange power. The basic idea is to relax one or more of the above constraints and find out the impact on the system. Since tie-line operation constraint is only related to the markets, we distinguish the results depending on whether tie-line operation constraint is considered or not.

There are 12 cases in total, which can be divided into two groups, with 6 cases in each group. In the first group, cases are based on the VRE capacity share and the consideration of tie-line operation constraint, as shown in Table. VII. Each case is composed of several scenarios, with each scenario considering the relaxation of a specific flexibility constraint. Under each scenario, the model in Section VII-A1) is conducted for all the days in the whole year and the annual indices are calculated.

To denote the effectiveness of the relaxation of flexibility constraints, we propose an indicator named 'VRE accommodation improvement ratio' (VAI) as:

$$VAI = (E_{\text{cons}}^{\text{VRE}} / E_{0\text{cons}}^{\text{VRE}} - 1) \times 100\% \quad (8)$$

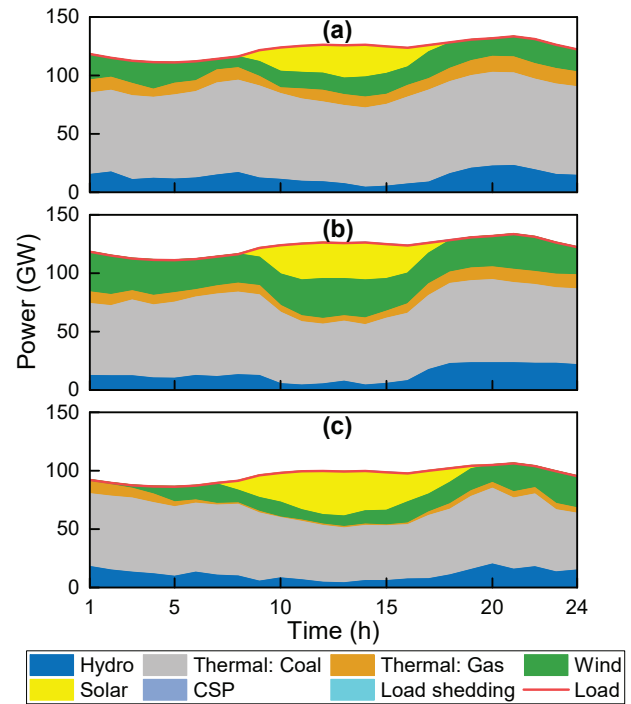


Fig. 10. The operation simulation results for the days: (a) with maximum daily demand, (b) with maximum wind generation, (c) with maximum PV generation.

TABLE VII
THE FIRST GROUP FOR THE EVALUATION OF FLEXIBILITY

VRE capacity%	38.20%	55.28%	64.97%
Consider tie-line operation constraint?	Yes(#1)	Yes(#2)	Yes(#3)
	No(#4)	No(#5)	No(#6)

The number in the bracket indicates the case number.

where $E_{0\text{cons}}^{\text{VRE}}$ and $E_{\text{cons}}^{\text{VRE}}$ represent the consumed VRE energy before and after one or more flexibility constraints are relaxed, respectively.

In the second group, for the investigation of the interaction between flexibility constraints, two flexibility constraints are relaxed simultaneously, with one of the constraints assigned as the minimum stable level of conventional units, VRE integration grid capacity or regional transmission grid capacity, respectively, as shown in Table. VIII. Similarly, each case involves several scenarios and the indices for each scenario are calculated by conducting the operation simulation model for all the 365 days. To investigate the extra VRE accommodation when the combination of constraints is relaxed, we propose the *Collaboration Benefit* (CB) indicator as:

$$CB = [(E_{\text{con},i,j}^{\text{VRE}} - E_{\text{cons},i}^{\text{VRE}} - E_{\text{cons},j}^{\text{VRE}}) / E_{0\text{cons}}^{\text{VRE}} - 1] \times 100\% \quad (9)$$

where $E_{\text{cons},i}^{\text{VRE}}$ means the consumed VRE energy with the relaxation of constraint i .

2) *Results*: Fig. 11 shows the results of Case 1 to Case 6. The $E_{0\text{cons}}^{\text{VRE}}$ is set under the consideration of tie-line operation constraint. The constraints with '*' mean that the tie-line operation constraint is **not** considered. The effect of constraint relaxation raises with the increase of VRE penetration. The most important factors enhancing the VRE accommodation

TABLE VIII
THE SECOND GROUP FOR THE EVALUATION OF FLEXIBILITY

VRE capacity% =64.97%	A flexibility constraint is combined with		
	Min stable level constraint	Integration grid capacity constraint	Regional grid capacity constraint
Consider tie-line operation constraint?	Yes(#7)	Yes(#8)	Yes(#9)
	No(#10)	No(#11)	No(#12)

The number in the bracket indicates the case number.

are the inter-regional transfer, integration grid, conventional plant minimum stable level and regional transmission grid, according to Fig. 11.

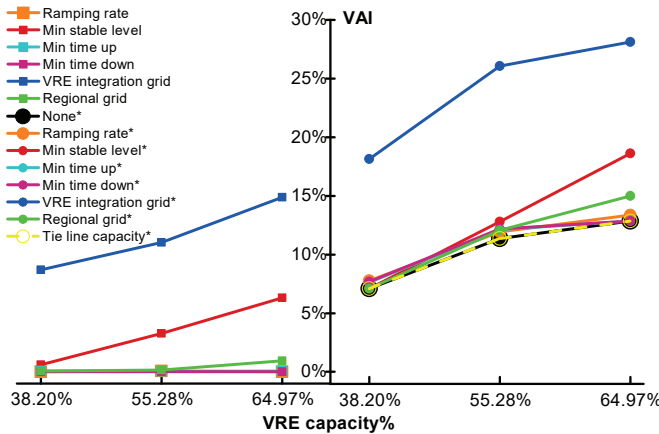


Fig. 11. Results of Case 1 to Case 6: Impact of individual flexibility factors on renewable accommodation.

In Fig. 12, the impact of the combination of flexibility constraints is illustrated. From Fig. 12 (a), the most effective way to improve VRE accommodation is the combination of VRE integration grid capacity and conventional unit minimum stable level constraints, followed by the combination of VRE integration grid capacity and regional transmission capacity constraints. Only these two combinations show obvious positive collaboration benefits. The results are similar when tie-line operation constraint is not considered (Fig. 12 (b)). When inter-regional transfers are promoted, the negative collaboration benefits decrease to nearly zero, showing the importance of the tie-line operation.

D. Flexibility Resource Planning

In this part, we investigate the optimized schemes of flexibility resources through three cases, using the model in section VII-A2). In the first case, the VRE capacity share is set as 38.20% and 64.97%, respectively. In the second case, the unit costs of battery and CAES are set as 80% and 120% of the reference value, respectively. In the last case, the unit compensation cost of DSR is set as 80% and 120% of the reference value, respectively. The latter two cases use a VRE capacity share of 64.97%. The reference values referred here are provided along with the original test system.

The results are shown in Fig. 13. It can be seen from Fig. 13 (a) that all aspects of the generation, network, demand, energy storage and market contribute to the optimal scheme under a

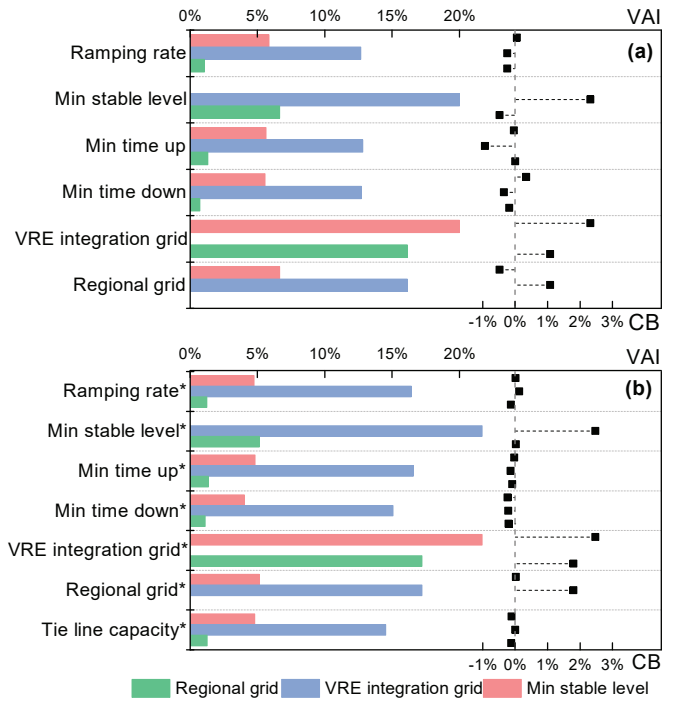


Fig. 12. Results of Case 7 to Case 12: Impact of the composition of flexibility factors on renewable accommodation.

high VRE penetration level. The thermal plant retrofit capacity is the main share when VRE penetration is not high, followed by that of the new AC & DC VRE integration lines. When the VRE capacity share reaches 64.97%, DC tie line, battery storage and DSR are deployed. Regarding costs (shown as points in Fig. 13 (a)), the retrofit cost and new line cost make up the most share when the VRE proportion is low, while they are far surpassed by the cost of battery storage when VRE penetration increases, which indicates that huge investment is required for the accommodation of VRE.

Fig. 13 (b) shows that the deployment of ES is closely related to its cost. If the unit capital cost decreases by 20%, the battery capacity will double to 9.5 GW (Fig. 13 (a)). While if the cost increases by 20%, the capacity will decrease to zero. Due to the high cost of CAES and pumped hydro, together with the fact that pumped hydro installation is closely dependent on the geographical environment, they are not invested in this case.

Fig. 13 (c) reveals that DSR shows low sensitivity to its compensation cost, but its cost impacts the deployment of ES. When the cost raises from 80% to 120% of the reference value, the capacity of DSR remains unchanged, while the ES capacity increases. The possible explanation is that, energy storage, which can also change the net load curve, is preferred for operation optimization, considering the increasing cost of DSR compensation.

VIII. DISCUSSIONS

There are some simplifications in the test system, such as the modeling of hydropower, the unit commitment problem and the DC power flow. Researchers can adapt the system and

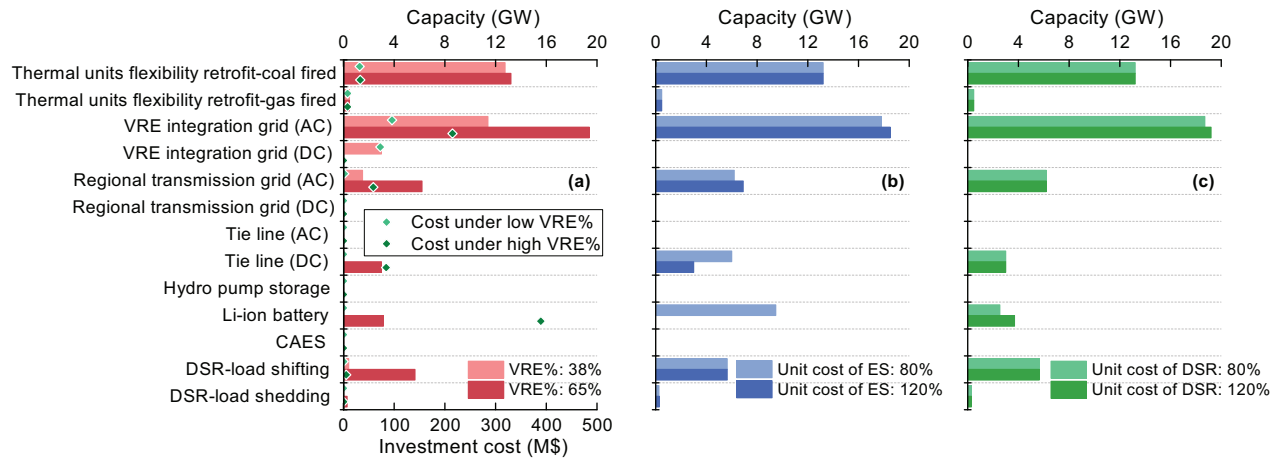


Fig. 13. The results of flexibility resource planning: the optimal allocation of multiple flexibility resources in all aspects of generation, network, demand, energy storage and market.

the modeling based on their requirements. Also, there are some advanced technologies like dynamic line rating, for researchers aiming to study the impact of dynamic line rating, they could adjust the data we provided to include dynamic line ratings.

Note that there are many standard adequacy studies conducted by utilities with detailed public available data [39], [40]. The data used in these works and ours have some similarities, but the goal of the studies are quite different. We focus on the flexibility to promote VRE accommodation rather than adequacy studies that focuses on reliability. We also conducted flexibility studies like investigating the collaboration benefit of multiple flexibility factors that would not be addressed in an adequacy study by utilities. Some new technologies like CSP and CAES are modeled in our system but are not considered in the current adequacy studies by utilities.

Flexibility is also important for the time scale smaller than 1 hour and we have also provided the sub-hourly data. Further studies like sub-hourly ramping, reserve and frequency regulation could be conducted based on this test system with necessary adaptations.

IX. CONCLUSIONS

System flexibility is becoming the focus of power system with variable renewable energy. To enable detailed studies, this paper presents a test system containing VRE integration grids, regional transmission grids and tie lines. Five sets of real-time series data of wind and PV power are provided with a resolution of finer than 15 min. The flexibility factors and resources are provided in all the generation, network, demand, energy storage and market side and classified in detail. The impacts of flexibility factors are analyzed, and the benchmarks of flexibility resource planning are provided.

Numerical results validate the “all hands-on deck” idea and indicate the importance of full network model by showing that (1) the VRE integration grid, unit minimum stable level, regional transmission grid and tie-line operation are the most influential factors to the flexibility; (2) combinations of the

above factors have positive collaboration benefits; (3) optimal flexibility schemes are provided from all the generation, network, demand and energy storage for the VRE accommodation.

REFERENCES

- [1] International Energy Agency (IEA), “Status of power system transformation 2019,” IEA, Report, 2019. [Online]. Available: <https://webstore.iea.org/status-of-power-system-transformation-2019-power-system-flexibility>
- [2] B. Mohandes, M. S. El Moursi, N. Hatziaargyriou, and S. El Khatib, “A review of power system flexibility with high penetration of renewables,” *IEEE Transactions on Power Systems*, vol. 34, no. 4, pp. 3140–3155, 2019.
- [3] M. Alizadeh, M. P. Moghaddam, N. Amjadi, P. Siano, and M. Sheikh-El-Eslami, “Flexibility in future power systems with high renewable penetration: A review,” *Renewable and Sustainable Energy Reviews*, vol. 57, pp. 1186–1193, 2016.
- [4] International Energy Agency (IEA), “World energy outlook 2018,” IEA, Report, 2018. [Online]. Available: <https://www.iea.org/reports/world-energy-outlook-2019>
- [5] International Energy Agency, “China power system transformation-assessing the benefit of optimised operations and advanced flexibility options,” IEA, Tech. Rep., 2019. [Online]. Available: <https://webstore.iea.org/china-power-system-transformation>
- [6] International Renewable Energy Agency (IRENA), “Power system flexibility for the energy transition,” IRENA, Report, 2018. [Online]. Available: <https://www.irena.org/publications/2018/Nov/Power-system-flexibility-for-the-energy-transition>
- [7] P. D. Lund, J. Lindgren, J. Mikkola, and J. Salpakari, “Review of energy system flexibility measures to enable high levels of variable renewable electricity,” *Renewable and Sustainable Energy Reviews*, vol. 45, pp. 785–807, 2015.
- [8] H. Kondziella and T. Bruckner, “Flexibility requirements of renewable energy based electricity systems—a review of research results and methodologies,” *Renewable and Sustainable Energy Reviews*, vol. 53, pp. 10–22, 2016.
- [9] International Renewable Energy Agency (IRENA), “Innovation landscape for a renewable-powered future,” IRENA, Report, 2019. [Online]. Available: <https://www.irena.org/publications/2019/Feb/Innovation-landscape-for-a-renewable-powered-future>
- [10] R. Villasana, L. Garver, and S. Salon, “Transmission network planning using linear programming,” *IEEE transactions on power apparatus and systems*, no. 2, pp. 349–356, 1985.
- [11] P. M. Subcommittee, “Ieee reliability test system,” *IEEE Transactions on power apparatus and systems*, no. 6, pp. 2047–2054, 1979.

- [12] C. Grigg, P. Wong, P. Albrecht, R. Allan, M. Bhavaraju, R. Billinton, Q. Chen, C. Fong, S. Haddad, S. Kuruganty *et al.*, "The IEEE reliability test system-1996. a report prepared by the reliability test system task force of the application of probability methods subcommittee," *IEEE Transactions on power systems*, vol. 14, no. 3, pp. 1010–1020, 1999.
- [13] J. Aghaei, A. Nikoobakht, M. Mardaneh, M. Shafie-khah, and J. P. Catalão, "Transmission switching, demand response and energy storage systems in an innovative integrated scheme for managing the uncertainty of wind power generation," *International Journal of Electrical Power & Energy Systems*, vol. 98, pp. 72–84, 2018.
- [14] Y. V. Makarov, C. Loutan, J. Ma, and P. De Mello, "Operational impacts of wind generation on California power systems," *IEEE transactions on power systems*, vol. 24, no. 2, pp. 1039–1050, 2009.
- [15] M. Ali, J. Ekström, and M. Lehtonen, "Sizing hydrogen energy storage in consideration of demand response in highly renewable generation power systems," *Energies*, vol. 11, no. 5, p. 1113, 2018.
- [16] B. Hua, R. Baldick, and J. Wang, "Representing operational flexibility in generation expansion planning through convex relaxation of unit commitment," *IEEE Transactions on Power Systems*, vol. 33, no. 2, pp. 2272–2281, 2017.
- [17] J. E. Price and J. Goodin, "Reduced network modeling of wecc as a market design prototype," in *2011 IEEE Power and Energy Society General Meeting*. IEEE, 2011, pp. 1–6.
- [18] J. M. Alemany, B. Arendarski, P. Lombardi, and P. Komarnicki, "Accentuating the renewable energy exploitation: Evaluation of flexibility options," *International Journal of Electrical Power & Energy Systems*, vol. 102, pp. 131–151, 2018.
- [19] M. Kristiansen, M. Korpås, and H. G. Svendsen, "A generic framework for power system flexibility analysis using cooperative game theory," *Applied energy*, vol. 212, pp. 223–232, 2018.
- [20] I. Pena, C. B. Martinez-Anido, and B.-M. Hodge, "An extended IEEE 118-bus test system with high renewable penetration," *IEEE Transactions on Power Systems*, vol. 33, no. 1, pp. 281–289, 2017.
- [21] J. Wang, J. Wei, Y. Zhu, and X. Wang, "The reliability and operation test system of power grid with large-scale renewable integration," *CSEE Journal of power and energy systems*, 2019.
- [22] Z. Zhuo, N. Zhang, J. Yang, C. Kang, C. Smith, M. Omalley, and B. Kroposki, "Transmission expansion planning test system for ac/dc hybrid grid with high variable renewable energy penetration," *IEEE Transactions on Power Systems*, 2019.
- [23] C. Barrows, A. Bloom, A. Ehlen, J. Ikaheimo, J. Jorgenson, D. Krishnamurthy, J. Lau, B. McBennett, M. O'Connell, E. Preston *et al.*, "The IEEE reliability test system: A proposed 2019 update," *IEEE Transactions on Power Systems*, 2019.
- [24] L. Gan, G. Li, and M. Zhou, "Coordinated planning of large-scale wind farm integration system and regional transmission network considering static voltage stability constraints," *Electric Power Systems Research*, vol. 136, pp. 298–308, 2016.
- [25] R. Hermes, T. Paulun, and H.-J. Haubrich, "Economic evaluation of large-scale wind integration in transmission networks," in *2008 IEEE/PES Transmission and Distribution Conference and Exposition*. IEEE, 2008, pp. 1–6.
- [26] H. Li, Z. Lu, Y. Qiao, and B. Zhang, "Flexibility test system," 2020. [Online]. Available: https://github.com/HaoLi9401/Dataset_of_flexibility_test_system_FTS-213
- [27] R. Christie, "Power systems test case archive." 2020. [Online]. Available: http://labs.ece.uw.edu/pstca/pf300/pg_tca300bus.htm
- [28] J. McCalley, J. Caspary, C. Clack, W. Galli, M. Marquis, D. Osborn, A. Orth, J. Sharp, V. Silva, and P. Zeng, "Wide-area planning of electric infrastructure: Assessing investment options for low-carbon futures," *IEEE Power and Energy Magazine*, vol. 15, no. 6, pp. 83–93, 2017.
- [29] E. Du, N. Zhang, B.-M. Hodge, C. Kang, B. Kroposki, and Q. Xia, "Economic justification of concentrating solar power in high renewable energy penetrated power systems," *Applied Energy*, vol. 222, pp. 649–661, 2018.
- [30] NREL, "System advisor model (sam)," 2020. [Online]. Available: <https://sam.nrel.gov/>
- [31] China Electricity Council, "National power reliability index in 2016," 2017. [Online]. Available: <https://cec.org.cn/detail/index.html?3-128991>
- [32] NREL, "Jedi transmission line model," 2020. [Online]. Available: <https://www.nrel.gov/analysis/jedi/transmission-line.html>
- [33] S. Venkataraman, G. Jordan, M. O'Connor, N. Kumar, S. Lefton, D. Lew, G. Brinkman, D. Palchak, and J. Cochran, "Cost-benefit analysis of flexibility retrofits for coal and gas-fueled power plants: August 2012–December 2013," National Renewable Energy Lab.(NREL), Golden, CO (United States), Tech. Rep., 2013.
- [34] N. Zhang, H. Dai, and Z. Hu, "A source-grid-load coordinated planning model considering system flexibility constraints and demand response," *Electric Power*, vol. 52, pp. 61–69, 2019.
- [35] K. Mongird, V. V. Viswanathan, P. J. Balducci, M. J. E. Alam, V. Fotedar, V. S. Koritarov, and B. Hadjerioua, "Energy storage technology and cost characterization report," Pacific Northwest National Lab.(PNNL), Richland, WA (United States), Tech. Rep., 2019.
- [36] W. J. Cole and A. Frazier, "Cost projections for utility-scale battery storage," National Renewable Energy Lab.(NREL), Golden, CO (United States), Tech. Rep., 2019.
- [37] L. Yang, C. Zhang, J. Jian, K. Meng, Y. Xu, and Z. Dong, "A novel projected two-binary-variable formulation for unit commitment in power systems," *Applied Energy*, vol. 187, pp. 732–745, 2017.
- [38] R. Hemmati, H. Saboori, and M. A. Jirdehi, "Stochastic planning and scheduling of energy storage systems for congestion management in electric power systems including renewable energy resources," *Energy*, vol. 133, pp. 380–387, 2017.
- [39] ENTSO-E, "Mid-term adequacy forecast – executive summary," 2020. [Online]. Available: <https://www.entsoe.eu/outlooks/midterm/>
- [40] RTE, "eco2mix," 2020. [Online]. Available: <https://www.rte-france.com/en/eco2mix>



Hao Li (S'18) received the B.S. degree in 2016 from North China Electric Power University, Beijing, China. He is currently working toward the Ph.D. degree at Tsinghua University. He is currently a visiting student in the Department of Electrical and Computer Engineering, University of Washington, Seattle, WA, USA.

His research interests include power system operation and planning, and renewable energy integration.

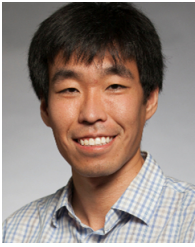


Zongxiang Lu (M'02–SM'18) received the B.S. and Ph.D. degrees in electrical engineering from Tsinghua University, Beijing, China, in 1998 and 2002, respectively. Since 2002, he has been with Tsinghua University, Beijing, China, where he is currently an Associate Professor of Electrical Engineering. He has been the PI of more than 40 academic and industrial projects. He is the author or co-author of 8 books, 29 international journal papers, and 78 Chinese journal papers on power system reliability, wind power integration, microgrid operation control, and smart grid, and so on. His research interests include large-scale wind power/PV stations integration analysis and control, energy and electricity strategy planning, power system reliability, DG, and microgrid. He is the Fellow of IET, and the Senior Member of IEEE and CSEE.



Ying Qiao (M'14) received the B.S. and Ph.D. degrees in electrical engineering from Shanghai Jiaotong University, Shanghai, China, and Tsinghua University, Beijing, China, in 2002 and 2008, respectively. Since 2010, she has been with Tsinghua University, where she is currently an Associate Professor of electrical engineering.

Her research interests include renewable energy and power system security and control.



Baosen Zhang received his Bachelor of Applied Science in Engineering Science degree from the University of Toronto in 2008; and his PhD degree in Electrical Engineering and Computer Sciences from University of California, Berkeley in 2013. He was a Postdoctoral Scholar at Stanford University.

He is currently an Assistant Professor in Electrical and Computer Engineering at the University of Washington, Seattle, WA. His research interests are in control, optimization and learning applied to power systems and other cyberphysical systems. He

received the NSF CAREER award as well as several best paper awards.



Yisha Lin (S'20) received the B.S. degree in electrical engineering from North China Electric Power University, Beijing, China, in 2018. She is currently working toward the Ph.D. degree at Tsinghua University.

Her major research interests include renewable energy integration and generation scheduling optimization.